Data-Driven Model-Free Adaptive Sliding Mode Control for Multi DC Motor Speed Regulation

Tony Blaise Bimenyimana[1], Dong Liu[1*], Yijie Yang[1]
1. College of Automation, Shenyang Aerospace University, Shenyang 110136, P. R. China
E-mail: 18804072112@163.com

Abstract: This paper proposes the distributed data-driven model-free adaptive sliding mode control method to solve the consensus problem of nonlinear multi-agent systems. Firstly, the equivalent data model for each agent is constructed using the compact-form dynamic linearization (CFDL) technique. Secondly, by utilizing process information from neighboring agents, the novel sliding surface is utilized to ensure the boundedness of the distributed measurement error. Subsequently, a distributed model-free adaptive sliding mode controller is developed for accurate consensus tracking. Finally, the effectiveness of the proposed control approach is validated through experiments on multi DC motor system.

Key Words: Data-driven control, model-free adaptive sliding mode control, nonlinear multi-agent systems, multi DC motor speed control.

1 Introduction

Multi-agent systems (MASs) consist of multiple interacting agents that cooperate to achieve a collective control objective. Such systems offer key benefits, including efficient decision-making, enhanced fault tolerance, and strong adaptability to dynamic environments. Due to the above characteristics, they have gained widespread attention in both theoretical and practical applications, such as sensor networks, transportation, agriculture, and industrial automation systems [1–3]. One of the fundamental challenges in multi-agent coordination is consensus tracking, aiming to enable all agents to synchronize to a common trajectory despite diverse initial states [4–8]. In practice, the distributed consensus problem is complicated by dynamic couplings among agents, communication constraints, and uncertain dynamics, which make it extremely difficult to establish accurate mathematical models. As a result, the above limitations in MAS interactions have motivated the development of data-driven control approaches.

The existing distributed control strategies [9–13] heavily rely on accurate system models to guarantee reliable performance and stability. However, with the continuous evolution of industrial processes and increasing system dynamics complexity, obtaining precise mathematical models becomes a challenging task. This modeling difficulty further limits the applicability of conventional methods in practical systems. Simultaneously, in modern industrial environments, large volumes of process information reflecting complex and uncertain system behaviors are continuously collected during operation. Leveraging such data for controller design has therefore become a promising alternative. In this context, to overcome modeling difficulties, model-free adaptive control (MFAC) [15–17] has emerged as an effective, practical and efficient solution, capable of achieving high-performance control without explicit modeling while adapting effectively to unknown and varying system dynamics.

Consequently, leveraging available data to achieve reliable consensus control has become a powerful research focus. Data-driven control [18–20] focuses on designing controllers utilizing I/O data solely. Various methods relying on measured data have been proposed, including model-free adaptive control, virtual reference feedback tuning [21], iterative learning control, PID control [22], data-driven predictive control, and others. Among them, MFAC [23–25] has shown strong significance in addressing the aforementioned challenges. The controller design process relies solely on I/O system information, thereby eliminating the need for accurate mathematical models. Moreover, MFAC has been implemented in various real-world applications, including motor systems, chemical processes, and industrial machinery, demonstrating strong adaptability and practical value.

Alternatively, sliding mode control [26] has emerged as a highly attractive approach for control researchers due to the robustness to parameter uncertainties and the capability to ensure fast responses. Currently, a new sliding mode control approach based on input-output data is presented in [27], eliminating the need for explicit system models. Although considerable progress in [28, 29] has been made in controlling nonlinear MASs, the dynamic couplings and complex nonlinear behaviors among agents [14] remain challenging in practical implementation.

However, the effectiveness of existing approaches [30–34] is limited in highly uncertain conditions because they typically rely on input-affine structures with known or partially known dynamics. Therefore, how to realize effective consensus tracking utilizing the model-free adaptive sliding mode control approach for nonlinear MASs remains an open question.

Taking the aforementioned considerations into account, this study proposes a data-driven model-free adaptive sliding mode control scheme for nonlinear multi-agent systems. This paper makes the following significant contributions:

1) Distributed model-free adaptive sliding mode control framework alongside a novel sliding surface is developed to ensure fast and robust consensus tracking in nonlinear MASs under uncertainties and disturbances constraints, thereby ensuring reliable cooperative behavior among agents.

2) Practical data-driven strategy is achieved using only input-output signals, ensuring bounded parameter adapta-

Funding for this research is supplied by the National Natural Science Foundation of China (62573304, 62273085 and 62473131) and the General Project of Education Department of Liaoning Province (JYTMS20230276).

tion and eliminating the need for explicit system models, which significantly enhances the usefulness of the proposed method in real-world applications.

The following sections outline the remaining content of this paper: The preliminaries together with the problem formulation are presented in Section II. Section III focuses on the development and discussion of the main results. Numerical simulations and performance analysis under various operating conditions are presented in Section IV. At the end, conclusions are summarized in Section V.

2 Preliminaries and problem formulation

2.1 Directed Graph Theory

The communication topology among agents is represented using the directed graph $\mathcal{G} = (\mathcal{V}, \mathcal{E}, \mathcal{A})$ to describe the information exchange. Here, $\mathcal{A} = [a_{ij}] \in \mathbb{R}^{N\times N}$ represents the adjacency matrix, the vertex set is defined as $\mathcal{V} = \{v_1, v_2, \ldots, v_N\}$, and $\mathcal{E} = [(v_j, v_i)|v_i \in \mathcal{V}] \subseteq \mathcal{V} \times \mathcal{V}$ is the set of edges. Moreover, $\mathcal{N}(i) = \{j \in \mathcal{V}|(i,j) \in \mathcal{E}\}$ denotes the neighbor set of agent i, where $a_{ij} \neq 0$. In this work, self-loop is allowed, which means $(i,i) \notin \mathcal{E}$ for any $i \in \mathcal{V}$, $a_{ii} = 0$. Furthermore, the degree matrix $K = diag(k_1, \ldots, k_N)$. Where $k_i > 0$ indicates that agent i can directly access data from the leader, meanwhile the Laplacian matrix L is constructed as the difference between the degree matrix $\mathcal{D}$ and the adjacency matrix $\mathcal{A}$, here $\mathcal{D} = diag(d_1, \ldots, d_N)$ and $d_i = \sum_{j=1}^{N} a_{ij}$ denotes the in-degree matrix. Moreover, it is assumed that the graph satisfies strong connectivity if the path exists between every pair of vertices.

2.2 Problem Formulation

A class of nonlinear multi-agent systems is defined and described below:

$$y_i(k+1) = f_i(y_i(k), u_i(k)), \quad i = 1, 2, \ldots, N \tag{1}$$

where $u_i(k) \in \mathbb{R}$ and $y_i(k) \in \mathbb{R}$ represent the system input and output signals of agent i, respectively. $f_i(\cdot)$ signifies an unknown nonlinear function.

Assumption 1: It is assumed that $\frac{\partial f(\cdot)}{\partial u_i(k)}$ is continuous.

Assumption 2: The generalized Lipschitz condition holds for the system (1), meaning that if $\Delta u_i(k) = u_i(k) - u_i(k-1) \neq 0$ then $|\Delta y_i(k+1)| \leq b|\Delta u_i(k)|$ holds for each time step k, where $\Delta y_i(k+1) = y_i(k+1) - y_i(k)$.

Remark 1: The above assumptions are general and commonly adopted in data-driven control. Specifically, Assumption 1 represents a general condition applicable to common nonlinear systems, whereas Assumption 2 implies that the change rate of the system input constrains the rate of change of the system output. In practice, the finite actuator capability in real systems ensures that the output variation remains bounded.

Assumption 3: A strongly connected communication graph $\mathcal{G}$ is assumed, which ensures that all followers can directly receive information from at least one leader [6].

Lemma 1 [8]: Consider the nonlinear multi-agent system (1) satisfying the above three assumptions. If $|\Delta u_i(k)| \neq 0$ holds, then the system dynamics can be represented using the CFDL data model as follows:

$$\Delta y_i(k+1) = \phi_i(k)\Delta u_i(k) \tag{2}$$

where $\phi_i(k)$ denotes pseudo partial derivative (PPD), satisfying $|\phi_i(k)| \leq b$.

The distributed measurement error of $\xi_i(k)$ for N agents is established as:

$$\xi_i(k) = \sum_{j\in N_i} a_{ij}(y_j(k) - y_i(k)) + d_i(y_d(k) - y_i(k)) \tag{3}$$

where $d_i = 1$ if agent i has direct to the leader information, otherwise $d_i = 0$. Additionally, $y_d(k)$ represents the reference trajectory.

Remark 2: No prior information about the system dynamics is required for the CFDL model (2). The time-varying PPD $\phi_i(k)$ is an inherent concept of the MFAC framework, which reflects the local input-output sensitivity using only measured data. Since the dynamic behavior of the PPD may be highly complex and difficult to analyze directly, employing a purely data-driven approach to estimate the numerical characteristics of $\phi_i(k)$ becomes a preferred solution for adaptive controller design.

3 Main Results

For clarity, this section consists of two parts. The first part presents the model-free adaptive sliding mode controller with improved tracking effectiveness. The second part provides the stability analysis, where the inductive assumption method is used to prove that both the distributed measurement error and parameter estimation error remain bounded. Moreover, the proposed control strategy is summarized in the overall block diagram illustrated in Fig. 1.

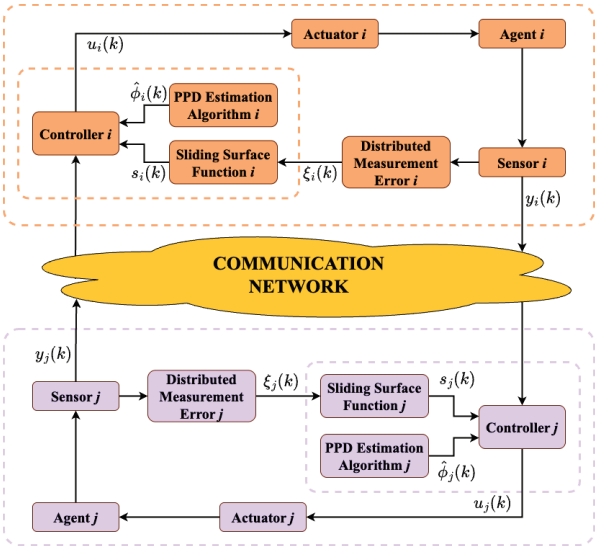

Fig. 1: Block diagram.

3.1 Model-Free Adaptive Sliding Mode Controller Design

Consider the following PPD criterion function for the parameter with unknown dynamics in (2):

$$J(\phi_i(k)) = |\Delta y_i(k) - \phi_i(k)\Delta u_i(k-1)|^2 + \mu|\phi_i(k) - \hat{\phi}_i(k-1)|^2 \tag{4}$$

By utilizing the optimal condition $\frac{\partial J(\phi_i(k))}{\partial \phi_i(k)} = 0$, the updating law with reset algorithm is derived:

$$\hat{\phi}_i(k) = \hat{\phi}_i(k-1) + \frac{\eta \Delta u_i(k-1)}{\mu + \Delta u_i(k-1)^2}(\Delta y_i(k) - \hat{\phi}_i(k-1)\Delta u_i(k-1)) \tag{5}$$

$$\hat{\phi}_i(k) = \hat{\phi}_i(1), \text{ if } |\hat{\phi}_i(k)| \leq \epsilon \; or \; sign(\hat{\phi}_i(k)) \neq sign(\hat{\phi}_i(1)) \tag{6}$$

herein, $\eta \in (0,1)$, $\mu > 0$ represents a positive weight factor. Additionally, ϵ is a small positive number and $\hat{\phi}_i(k)$ signifies the estimated value of $\phi_i(k)$.

To design the MFAC control algorithm, the pseudo partial derivative $\hat{\phi}_i(k)$ is estimated using the update law (5). Subsequently, the following MFAC algorithm is implemented:

$$\Delta u_{i,\text{MFA}}(k) = \frac{\rho \hat{\phi}_i(k)}{\lambda + \hat{\phi}_i(k)^2}\xi_i(k) \tag{7}$$

where ρ denotes the step size constant and $\lambda > 0$.

Toward the design of the sliding mode controller, the sliding surface function is described by:

$$s_i(k) = \alpha \xi_i(k) - \xi_i(k-1) \tag{8}$$

where $\alpha > 1$ represents a positive constant.

Accordingly, the expression (3) is then updated as

$$\xi_i(k+1) = \xi_i(k) - (\sum_{j \in N_i} a_{ij} + d_i)\phi_i(k)\Delta u_i(k) + \sum_{j \in N_i} a_{ij}\Delta y_j(k) + d_i \Delta y_d(k+1) \tag{9}$$

wherein $\Delta y_j(k+1)$ is replaced with $\Delta y_j(k)$ because the data at the next moment cannot be obtained.

Therefore, by applying the reaching condition $s_i(k+1) = 0$ leads to the subsequent equivalent control law.

$$\Delta u^e_{i,\text{SM}}(k) = \frac{\omega \hat{\phi}_i(k)}{\sigma + \hat{\phi}_i(k)^2}\left(\frac{\xi_i(k) + \sum_{j \in N_i} a_{ij}\Delta y_j(k)}{\sum_{j \in N_i} a_{ij} + d_i} + \frac{d_i \Delta y_d(k+1)}{\sum_{j \in N_i} a_{ij} + d_i} - \frac{\xi_i(k)}{\alpha(\sum_{j \in N_i} a_{ij} + d_i)}\right) \tag{10}$$

The controller consists of an equivalent control law and switching control law, which means:

$$\Delta u_{i,\text{SM}}(k) = \Delta u^e_{i,\text{SM}}(k) + \Delta u^s_{i,\text{SM}}(k) \tag{11}$$

Besides, the switching control law $\Delta u^s_{i,\text{SM}}(k)$ is presented:

$$\Delta u^s_{i,\text{SM}}(k) = \frac{\omega \hat{\phi}_i(k)}{\sigma + \hat{\phi}_i(k)^2}\tau_s sign(s_i(k)) \tag{12}$$

where $\tau_s > 0$ denotes the switching gain of the sliding mode controller that regulates the convergence rate of the sliding surface.

As a consequence, taking into consideration (10), (11) and (12), the controller is summarized as follows:

$$\Delta u_{i,\text{SM}}(k) = \frac{\omega \hat{\phi}_i(k)}{\sigma + \hat{\phi}_i(k)^2}\left(\frac{\xi_i(k) + \sum_{j \in N_i} a_{ij}\Delta y_j(k)}{\sum_{j \in N_i} a_{ij} + d_i} + \frac{d_i \Delta y_d(k+1)}{\sum_{j \in N_i} a_{ij} + d_i} - \frac{\xi_i(k)}{\alpha(\sum_{j \in N_i} a_{ij} + d_i)}\right) + \tau_s sign(s_i(k)) \tag{13}$$

Subsequently, the final input is given by

$$u_i(k) = u_i(k-1) + \Delta u_{i,\text{MFA}}(k) + \Gamma_i \Delta u_{i,\text{SM}}(k) \tag{14}$$

where the parameter Γ_i is a gain factor selected through parameter tuning. It determines the contribution of the sliding mode control term in the final control input and is chosen to balance tracking accuracy and control performance; larger values improve robustness, while smaller values reduce oscillations.

3.2 Stability Analysis

Theorem 1: Let the system (1) satisfy assumptions 1-3. Using the designed algorithms (5) together with the reset condition (6), the sliding surface (8) and controller (13) guarantee that $\hat{\phi}_i(k)$ remains bounded. Simultaneously, the distributed measurement error is also bounded.

Proof: The analysis proceeds by proving the boundedness of $\tilde{\phi}_i(k)$, and ensure that $\xi_i(k)$ remains bounded, respectively.

Part i: First, define the PPD estimation error as $\tilde{\phi}_i(k) = \hat{\phi}_i(k) - \phi_i(k)$. By substituting the adaptive update law (5), the following result is derived:

$$\begin{aligned}\tilde{\phi}_i(k) &= \tilde{\phi}_i(k-1) + \frac{\eta \Delta u_i(k-1)}{\mu + \Delta u_i(k-1)^2}(\phi_i(k-1) \\ &\quad \Delta u_i(k-1) - \hat{\phi}_i(k-1)\Delta u_i(k-1)) \\ &\quad - \phi_i(k) + \phi_i(k-1) \\ &= \left(1 - \frac{\eta \Delta u_i(k-1)^2}{\mu + \Delta u_i(k-1)^2}\right)\tilde{\phi}_i(k-1) - \Delta \phi_i(k)\end{aligned} \tag{15}$$

Denote that the term $\frac{\eta |\Delta u_i(k-1)|^2}{\mu + |\Delta u_i(k-1)|^2}$ exhibits a monotonic increase with respect to $|\Delta u_i(k-1)|^2$, and bounded below by $\frac{\eta \epsilon^2}{\mu + \epsilon^2}$. As a consequence, a scalar constant $q_1 \in (0,1)$ can be identified such that $0 < \eta \leq 1$ and $\mu > 0$.

$$0 < \left|1 - \frac{\eta \Delta u_i(k-1)^2}{\mu + \Delta u_i(k-1)^2}\right| \leq 1 - \frac{\eta \epsilon^2}{\mu + \epsilon^2} = q_1 < 1 \tag{16}$$

Because of $|\phi_i(k)| < \bar{d}$, and $|\Delta \phi_i(k)| < 2\bar{d}$, the following equation (15) can be represented as:

$$\begin{aligned}|\tilde{\phi}_i(k)| &\leq q_1 |\tilde{\phi}_i(k-1)| + 2\bar{d} \\ &\leq q_1^2 |\tilde{\phi}_i(k-2)| + 2q_1\bar{d} + 2\bar{d} \\ &\vdots \\ &\leq q_1^{k-1}|\tilde{\phi}_i(1)| + \frac{2\bar{d}}{1-q_1}(1 - q_1^{k-1})\end{aligned} \tag{17}$$

which implies $\tilde{\phi}_i(k)$ remains bounded, given that the boundedness of $\phi_i(k)$ is ensured by Lemma 1.

Part ii: Next, the boundedness of $\xi_i(k)$.

By incorporating (5) into (9), the updated equation of $\xi_i(k+1)$ can be expressed as:

$$\begin{aligned}
\xi_i(k+1) &= \xi_i(k) + \sum_{j\in N_i} a_{ij}\Delta y_j(k) + d_i\Delta y_d(k+1) \\
&\quad - \frac{\omega\phi_i(k)\hat{\phi}_i(k)}{\sigma+\hat{\phi}_i(k)^2}(1-\frac{1}{\alpha})\xi_i(k) - \frac{\omega\phi_i(k)\hat{\phi}_i(k)}{\sigma+\hat{\phi}_i(k)^2} \\
&\quad \sum_{j\in N_i} a_{ij}\Delta y_j(k) - \frac{\omega\phi_i(k)\hat{\phi}_i(k)}{\sigma+\hat{\phi}_i(k)^2} d_i\Delta y_d(k+1) \\
&\quad + (\sum_{j\in N_i} a_{ij} + d_i)\tau_s sign(s_i(k)) \\
&= \left(1 - \frac{\omega\phi_i(k)\hat{\phi}_i(k)}{\sigma+\hat{\phi}_i(k)^2}(1-\frac{1}{\alpha})\right)\xi_i(k) \\
&\quad + \left(1 - \frac{\omega\phi_i(k)\hat{\phi}_i(k)}{\sigma+\hat{\phi}_i(k)^2}\right)(\sum_{j\in N_i} a_{ij}\Delta y_j(k) \\
&\quad + d_i\Delta y_d(k+1)) - \frac{\omega\phi_i(k)\hat{\phi}_i(k)}{\sigma+\hat{\phi}_i(k)^2} \\
&\quad (\sum_{j\in N_i} a_{ij} + d_i)\tau_s sign(s_i(k)) \qquad (18)
\end{aligned}$$

Subsequently, take $0 < h_0 < h_i(k) < \frac{\omega b}{2\sqrt{\sigma}} < 1$ into consideration, wherein

$$\begin{cases}
\phi_i(k) < b \\
h_i(k) = \dfrac{\omega\phi_i(k)\hat{\phi}_i(k)}{\sigma+\hat{\phi}_i(k)^2} \\
g_i(k) = (1-h_i(k))(\sum_{j\in N_i} a_{ij} + d_i)\Delta y_d(k+1) \\
\qquad - h_i(k)(\sum_{j\in N_i} a_{ij} + d_i)\tau_s\, sign(s_i(k)) \\
|g_i(k)| < g_0
\end{cases}$$

The following inequality is obtained by taking the absolute value of each term of (18).

$$\begin{aligned}
|\xi_i(k+1)| &\le |1-h_i(k)(1-\frac{1}{\alpha})||\xi_i(k)| + |g_i(k)| \\
&\le |1-h_i(k)(1-\frac{1}{\alpha})||\xi_i(k)| + g_0(k) \\
&\ \ \vdots \\
&\le 1 - h_0(1-\frac{1}{\alpha})^k|\xi_i(0)| + g_0(2-h_0(1-\frac{1}{\alpha})) \\
& \qquad (19)
\end{aligned}$$

Therefore, the following result will be given as

$$\lim_{k\to\infty} \xi_i(k) = \frac{\alpha g_0}{(\alpha-1)h_0} \qquad (20)$$

In summary, both the parameter estimation $\hat{\phi}_i(k)$ and the measurement error $\xi_i(k)$ remain bounded under the proposed adaptive sliding mode control scheme. The condition $0 < h_0 < h_i(k) < \frac{\omega b}{2\sqrt{\sigma}} < 1$ ensures that the adaptive parameters are stable, thereby enabling effective performance of the distributed controller. This concludes the proof.

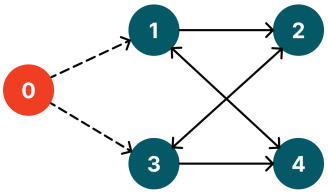

Fig. 2: Communication topology among agents.

4 Simulation Example

This section describes the usefulness of the provided control approach, which is validated by both numerical simulations and physical experimental verification. The DC brushed motors supplied at 12V with a no-load speed of 293±21RPM and a gear ratio of 20, providing increased torque. Hall encoders with 13 pulses per revolution are used to capture rotor motion. The motor speed is measured in revolutions per second (r/s) based on encoder measurements and the sampling interval t. The total number of encoder counts per revolution is calculated as $rT = 4N_eRr$, where N_e is the encoder line count equal to 13, R_r is the reduction ratio equal to 20. The number of rotations is determined using $N_r = \frac{m}{rT}$, with m representing the total encoder count. For each agent, the output data model is governed by:

$$y_i(k+1) = 0.5y_i(k) + b_iu_i(k) - 0.02y_i(k)^{p_i} + 0.45$$

Noting that the multi-agent systems are heterogeneous, with four agents exhibit distinct dynamic models. In addition, these models are not used in the control design but used solely for generating the input and output data required for the MAS simulations. As illustrated in Fig. 2, vertex 0 represents the virtual leader. Reception of the leader information occurs solely at agents 1 and 3, forming a strongly connected communication graph. For the considered graph, the Laplacian matrix is expressed below:

$$L = \begin{bmatrix} 1 & 0 & 0 & -1 \\ -1 & 2 & -1 & 0 \\ 0 & -1 & 1 & 0 \\ -1 & 0 & -1 & 2 \end{bmatrix}$$

with $D = \text{diag}(1,0,1,0)$.

Example 1: In this case study, the reference trajectory is a time-invariant signal $y_d(k) = 0.6$. The initial parameters are set as $u_i(1) = 0$, $y_i(1) = 0$, and $\hat{\phi}_i(1) = 1$ for all agents in this simulation. The control gains are set as $\Gamma_1 = \Gamma_3 = 0.45$ and $\Gamma_2 = \Gamma_4 = 0.15$. The system model parameters include $[b_1, b_2, b_3, b_4] = [\frac{6m}{rT}, \frac{5.75m}{rT}, \frac{6m}{rT}, \frac{5.75m}{rT}]$ and $[p_1, p_2, p_3, p_4] = [3, 2, 3, 2], m = 600, r_T = 1024$. Other parameters are $\tau_s = 10^{-5}$, $\eta = 1$, $\mu = 0.005$, $\rho = 7.5$, $\lambda = 350$, $\omega = 10$, $\sigma = 95$, $\alpha = 15$, and $\epsilon = 10^{-5}$.

The method [1] adopts a model-free adaptive control framework for multi-agent consensus tracking. In contrast, the proposed approach introduces a distributed data-driven model-free adaptive sliding mode control strategy, which incorporates a novel sliding surface and adaptive gain mechanism to improve robustness and convergence performance. Therefore, the following simulations compare the proposed scheme with method [1] to demonstrate the effectiveness and performance advantages of the developed scheme.

Fig. 3 presents the proposed scheme achieves superior control performance compared to method [1]. As shown in the below figure, the proposed method ensures faster convergence, smaller overshoot, and improved steady-state tracking accuracy. While method [1] exhibits the oscillations and slower response in transient phase, this highlights the stronger adaptability and robustness of the proposed method. Moreover, Fig. 4 illustrates the distributed measurement errors, which remain interval within the range of [-0.02, 0.02], demonstrating the proposed control strategy capability.

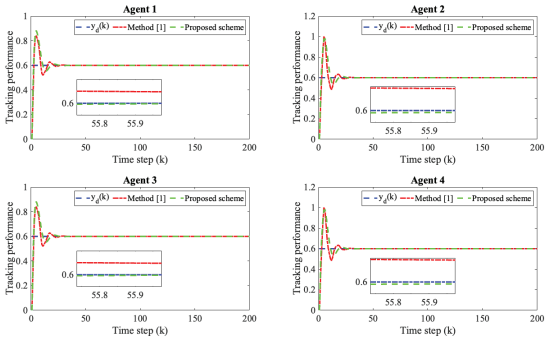

Fig. 3: Tracking response for the time-invariant reference trajectory.

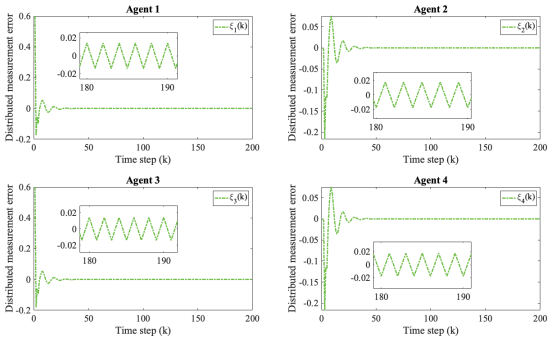

Fig. 4: Distributed measurement errors for the time-invariant reference trajectory.

The effectiveness of the developed method is quantified by calculating the mean square error (MSE) for each agent. The MSE values are presented in Table 1. For each follower agent, the MSE is determined using the following formula:

$$\text{MSE}_i(k) = \frac{1}{m}\sum_{k=1}^{m} \xi_i^2(k)$$

wherein m indicates the overall number of sampling steps. In comparison to the existing approach [1], the developed strategy demonstrates significant improvement in accuracy, reducing the average MSE across agents by a factor of approximately 1.29. This notable reduction confirms the effectiveness of the proposed technique.

Example 2: The expression for the reference trajectory is:

$$y_d(k) = 0.6\sin(0.07\pi(k)) + 0.6\cos(0.04\pi(k)), k \in [0, 200]$$

Table 1: Comparison of mean squared error (Example 1)

$\text{MSE}_i(k)$	Method [1]	Proposed scheme
Follower 1	4.9135×10^{-3}	4.0732×10^{-3}
Follower 2	3.2197×10^{-3}	2.2558×10^{-3}
Follower 3	4.9135×10^{-3}	4.0732×10^{-3}
Follower 4	3.2197×10^{-3}	2.2558×10^{-3}
Average	4.0666×10^{-3}	3.1649×10^{-3}

Fig. 5 presents the tracking performance for the time-varying trajectory. All agents are able to track the time-varying reference trajectory. Compared to the existing method [1], the proposed scheme achieves the faster response, reduced steady-state error, and improved tracking accuracy.

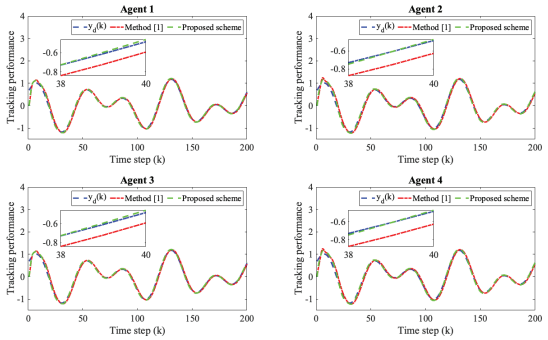

Fig. 5: Tracking response for the time-variant reference trajectory.

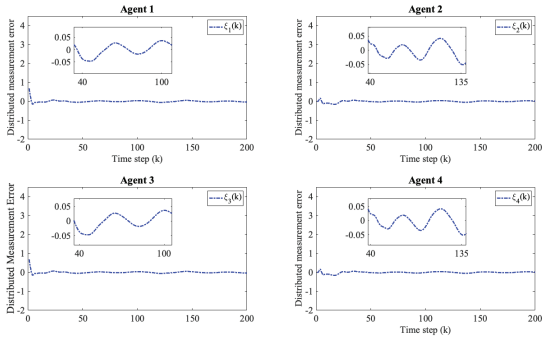

Fig. 6: Distributed measurement errors for the time-variant reference trajectory.

As highlighted, the proposed approach closely follows the reference trajectory, whereas method [1] exhibits the deviations and slower error convergence. Additionally, as shown in Fig. 6 the error among agents are bounded. Therefore, the proposed method demonstrates superior adaptability under time-varying conditions, ensuring high-performance tracking. For time-varying reference trajectories, the mean squared errors of distributed measurements for two control strategies are detailed in Table 2. Relative to the conventional approach [1], the proposed scheme reduces in average MSE by approximately 1.16.

To verify practical feasibility, the proposed consensus tracking control methodology is implemented on a multi DC

Table 2: Comparison of mean squared error (Example 2)

$\mathrm{MSE}_i(k)$	Method [1]	Proposed scheme
Follower 1	2.8319×10^{-3}	2.6984×10^{-3}
Follower 2	1.4561×10^{-3}	9.8907×10^{-4}
Follower 3	2.8319×10^{-3}	2.6984×10^{-3}
Follower 4	1.4561×10^{-3}	9.8907×10^{-4}
Average	2.1445×10^{-3}	1.8432×10^{-3}

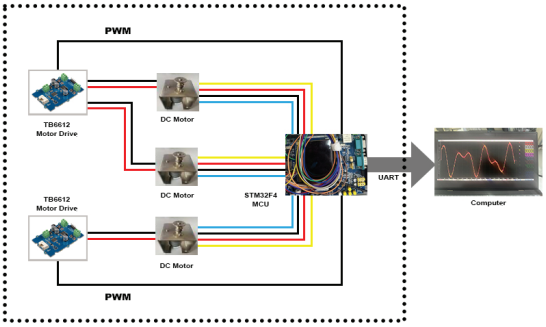

Fig. 7: System connection diagram of multi DC motor consensus tracking control.

motor experimental platform, as demonstrated in Fig. 8. The system setup comprises three DC motors equipped with Hall encoders and reduction gears, an STM32F407 main control chip, two motor drive modules, and a liquid crystal display (LCD) module. The microcontroller unit STM32F407ZGT6 is used for high-resolution pulse width modulation output generation to achieve precise motor speed control. The timer module is utilized for this purpose.

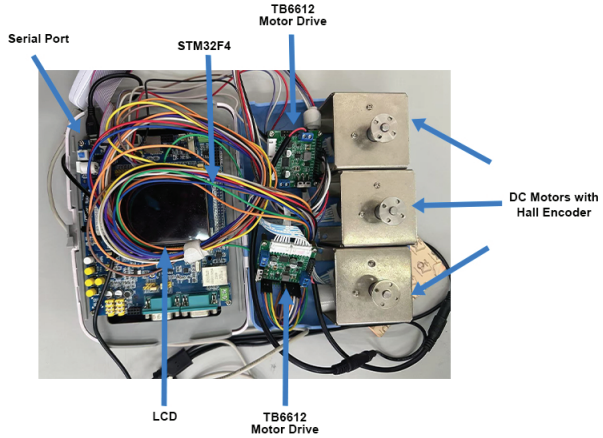

Fig. 8: Multi DC motor system.

In addition, the controller code is written in C language using STM32CubeIDE, while STM32CubeMX is used for pin configuration, where the experiment aims to confirm that the three motors accurately track the reference trajectory:

Fig. 9 presents the speed tracking performance of multi DC motor demonstrating the proposed control technique performance. Overall, the simulation results suggest that the proposed control system is capable of tracking a constant desired trajectory for multiple agents. While initial transient errors may occur, the system ultimately achieves a steady-state condition with minimal tracking error. The variations in

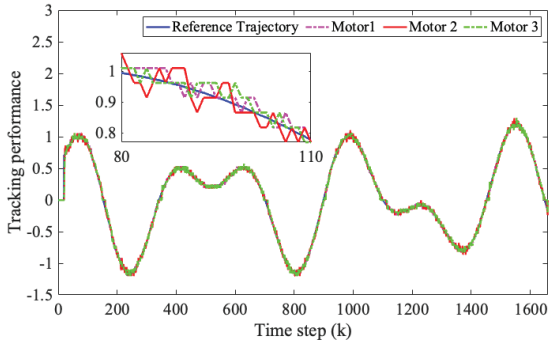

Fig. 9: Speed tracking performance of three DC motors.

tracking performance among the agents highlight the potential influence of individual characteristics and external factors.

The distributed errors for three DC motors result in mean squared errors of 1.0840×10^{-3}, 1.5036×10^{-3}, and 1.4887×10^{-3}, respectively. The average of 1.3588×10^{-3} demonstrates the validity of the proposed control strategy in practical applications. Meanwhile, the method consistently maintains mean squared error around 10^{-3}.

Remark 3: The parameters ρ and ω directly influence the robustness against system uncertainties and disturbances. Larger values can enhance disturbance rejection capability, but may also amplify the control effort. In addition, the sliding surface gain σ and the adaptive update gain α determine the convergence rate of the tracking error. Excessive values may cause chattering or oscillatory responses, whereas overly small values may slow the adaptation process. Therefore, selecting ρ and ω properly ensures a balance between robustness, convergence speed, and control smoothness.

5 Conclusion

In this paper, the model-free adaptive sliding mode control approach is presented to address the consensus problem of MASs. Firstly, each agent equivalent data model is obtained using the CFDL method. Secondly, a novel sliding surface is presented for the purpose of ensuring that the distributed measurement error is guaranteed remains bounded. Moreover, the developed strategy effectively mitigates the impact of distributed measurement errors across agents. The simulation results, quantitatively confirm the superiority of the proposed technique. Specifically, the mean squared error for each agent is calculated, revealing an average mean squared error reduction of approximately 1.29 compared to the existing approach [1], and approximately 1.16 for time-varying signals. Finally, the effectiveness of the presented control approach is further validated using physical experiments on multi DC motor system.

References

[1] X. Bu, Z. Hou, and H. Zhang, "Data-driven multiagentsystems consensus tracking using model free adaptive control," IEEE Transactions on Neural Networks and Learning Systems, vol. 29, no. 5, pp. 1514-1524, 2018.

[2] M. Parsa and M. Danesh, "Robust containment control of uncertain multi-agent systems with time-delay and heterogeneous lipschitz nonlinearity," IEEE Transactions on Systems,

Man, and Cybernetics: Systems, vol. 51, no. 4, pp. 2312-2321, 2021.
[3] A.-Y. Lu and G.-H. Yang, "Distributed secure state estimation for linear systems against malicious agents throughsorting and filtering," Automatica, vol. 151, pp. 110927,2023.
[4] T. Li, W. Bai, Q. Liu, Y. Long and C. L. P. Chen, "Distributed fault tolerant containment control protocols for the discrete-time multiagent systems via reinforcement learning method," IEEE Transactions on Neural Networks and Learning Systems, vol. 34, no. 8, pp. 3979-3991, Aug. 2023
[5] Y. Yang, Y. Xiao and T. Li, "Attacks on formation control for multiagent systems," IEEE Transactions on Cybernetics, vol. 52, no. 12, pp. 12805- 12817, Dec. 2022
[6] R. Olfati-Saber, J. A. Fax, and R. M. Murray, "Consensus and cooperation in networked multi-agent systems," *Proceedings of the IEEE*, vol. 95, no. 1, pp. 215-233, 2007.
[7] M. Sampei, T. Tamura, T. Kobayashi, and N. Shibui, "Arbitrary path tracking control of articulated vehicles using nonlinear control theory," IEEE Trans. Control Syst. Technol., vol. 3, no. 1, pp. 125-131, Mar. 1995.
[8] W. Ren, R. W. Beard, and E. M. Atkins, "Information consensus in multivehicle cooperative control," *IEEE Control Systems*, vol. 27, no. 2, pp. 71-82, 2007.
[9] D. Xu, B. Jiang, and P. Shi, "Adaptive observer based data-driven control for nonlinear discrete-time processes," *IEEE Transactions on Automation Science and Engineering*, vol. 11, no. 4, pp. 1037-1045, 2014.
[10] J. Wang, X. Wang, X. Zhang, and S. Zhu, "Global h-synchronization for high-order delayed inertial neural networks via direct SORS strategy," *IEEE Transactions on Systems, Man, and Cybernetics: Systems*, vol. 53, no. 11, pp. 6693-6704, 2023.
[11] F. Xu, X. Ruan, and X. Pan, "Event-triggered leaderfollowing consensus control of multiagent systems against DoS attacks," International Journal of Control, Automation and Systems, vol. 22, pp. 3424-3433, 2024.
[12] Y. Liu, L. Liu, and S. Tong, "Adaptive neural network tracking design for a class of uncertain nonlinear discrete time systems with dead-zone," Science China Information Sciences, vol. 57, pp. 1-12, 2014.
[13] Z. Dong, X. Wang, X. Zhang, M. Hu, and T.N. Dinh, "Global exponential synchronization of discrete-time high order switched neural networks and its application to multi channel audio encryption," Nonlinear Analysis: Hybrid systems, vol. 47, pp. 101291, 2023.
[14] X. Liu, J. Lam, W. Yu, and G. Chen, "Finite-time consensus of multiagent systems with a switching protocol," *IEEE Transactions on Neural Networks and Learning Systems*, vol. 27, no. 4, pp. 853-862, Apr. 2016.
[15] Z. Hou and Z. Wang, "From model-based control to data-driven control: Survey, classification and perspective," Inf. Sci., vol. 235, pp. 3-35, 2013.
[16] Z. Hou and S. Jin, "A novel data-driven control approach for a class of discrete-time nonlinear systems," IEEE Trans. Control Syst. Technol., vol. 19, no. 6, pp. 1549-1558, Nov. 2011.
[17] Y. Asadi, M.M. Farsangi, and M.H. Rezaei, "Improved data-driven adaptive control structure against input and output saturation," International Journal of Control, Automation and Systems, vol. 22, pp. 2981-2989, 2024.
[18] Y. Hui, R. Chi, B. Huang, Z. Hou, and S. Jin, "Observer-based sampled-data model-free adaptive control for continuous-time nonlinear nonaffine systems with input rate constraints," IEEE Transactions on Systems, Man, and Cybernetics: Systems, vol. 51, no. 12, pp. 7813-7822, 2021.
[19] Y.-S. Ma, W.-W. Che, C. Deng, and Z.-G. Wu, "Distributed model-free adaptive control for learning nonlinear MASs under DoS attacks," IEEE Transactions on Neural Networks and Learning Systems, vol. 34, no. 3, pp. 1146-1155, 2023.
[20] H. Wang, Q. Luo, N. Li, and W. Zheng, "Data-driven model free formation control for multi-USV system in complex marine environments," International Journal of Control, Automation and Systems, vol. 20, pp. 3666-3677, 2022.
[21] L. Duan, Z. Hou, X. Yu, S. Jin, and K. Lu, "Data-driven model-free adaptive attitude control approach for launch vehicle with virtual reference feedback parameters tuning method," IEEE Access, vol. 7, pp. 54106-54116, 2019.
[22] Kiam Heong Ang, G. Chong and Yun Li, "PID control system analysis, design, technology," IEEE Transactions on Control Systems Technology, vol. 13, no. 4, pp. 559-576, Jul. 2005.
[23] P. Zhu, S. Jin, X. Bu and Z. Hou, "Improved model-free adaptive control for MIMO nonlinear systems with event-triggered transmission scheme and quantization," IEEE Transactions on Cybernetics, vol. 53, no. 9, pp. 5867-5880, Sept. 2023.
[24] D. Xu, Y. Shi and Z. Ji, "Model-free adaptive discrete-time integral sliding-mode-constrained-control for autonomous 4WMV parking systems," IEEE Transactions on Industrial Electronics, vol. 65, no. 1, pp. 834-843, Jan. 2018.
[25] D. Liu and G.-H. Yang, "Prescribed performance model-free adaptive integral sliding mode control for discrete-time nonlinear systems," IEEE Transactions on Neural Networks and Learning Systems, vol. 30, no. 7, pp. 2222-2230, Jul. 2019.
[26] P. Shi, Y. Xia, G. Liu, D. Rees, On designing of sliding-mode control for stochastic jump systems, IEEE Trans. Automat. Control 51 (1) (2006) 97-103.
[27] D. Liu and G.-H. Yang, "Data-driven adaptive sliding mode control of nonlinear discrete-time systems with prescribed performance," IEEE Transactions on Systems, Man, and Cybernetics: Systems, vol. 49, no. 12, pp. 2598-2604, 2019.
[28] Z. Wu, X. Wang, and X. Zhao, "Backstepping terminal sliding mode control of DFIG for maximal wind energy captured," Int. J. Innovative Comput. Inf. Control, vol. 12, no. 5, pp. 1565-1579, 2016.
[29] X. Yan and C. Edwards, "Adaptive sliding-mode-observer-based fault reconstruction for nonlinear systems with parametric uncertainties," IEEE Trans. Ind. Electron., vol. 55, no. 11, pp. 4029-4036, Nov. 2008.
[30] J. Liu, W. Luo, X. Yang, and L. Wu, "Robust model-based fault diagnosis for PEM fuel cell air-feed system," IEEE Trans. Ind. Electron., vol. 63, no. 5, pp. 3261-3270, May 2016.
[31] A. Anuchin, A. Dianov and F. Briz, "Synchronous Constant Elapsed Time Speed Estimation Using Incremental Encoders," in IEEE/ASME Transactions on Mechatronics, vol. 24, no. 4, pp. 1893-1901, Aug. 2019, doi: 10.1109/TMECH.2019.2928950.
[32] S. Qin and T. Badgwell, "A survey of industrial model predictive control technology," Control Eng. Pract., vol. 11, pp. 733-764, 2003.
[33] X. Ma, F. Sun, H. Li, and B. He, "Neural-network-based integral sliding-mode tracking control of second-order multi-agent systems with unmatched disturbances and completely unknown dynamics," *International Journal of Control, Automation and Systems*, vol. 15, no. 4, pp. 1925-1935, 2017.
[34] R. Rahmani, H. Toshani, and S. Mobayen, "Consensus tracking of multi-agent systems using constrained neural-optimiser-based sliding mode control," *International Journal of Systems Science*, vol. 51, no. 14, pp. 2653-2674, 2020.